Allelic polymorphism of *GIGANTEA* is responsible for naturally occurring variation in circadian period in *Brassica rapa*

Qiguang Xie[a,1], Ping Lou[a,1], Victor Hermand[a], Rashid Aman[b], Hee Jin Park[b], Dae-Jin Yun[b], Woe Yeon Kim[b], Matti Juhani Salmela[c], Brent E. Ewers[c], Cynthia Weinig[c,d], Sarah L. Khan[a], D. Loring P. Schaible[a], and C. Robertson McClung[a,2]

[a]Department of Biological Sciences, Dartmouth College, Hanover, NH 03755-3563; [b]Division of Applied Life Science (BK21 Program), Plant Molecular Biology and Biotechnology Research Center and Institute of Agriculture and Life Sciences, Gyeongsang National University, Jinju 660–701, South Korea; and Departments of [c]Botany and [d]Molecular Biology, University of Wyoming, Laramie, WY 82071

Edited by Susan S. Golden, University of California, San Diego, La Jolla, CA, and approved February 10, 2015 (received for review November 13, 2014)

***GIGANTEA* (*GI*) was originally identified by a late-flowering mutant in *Arabidopsis*, but subsequently has been shown to act in circadian period determination, light inhibition of hypocotyl elongation, and responses to multiple abiotic stresses, including tolerance to high salt and cold (freezing) temperature. Genetic mapping and analysis of families of heterogeneous inbred lines showed that natural variation in *GI* is responsible for a major quantitative trait locus in circadian period in *Brassica rapa*. We confirmed this conclusion by transgenic rescue of an *Arabidopsis gi-201* loss of function mutant. The two *B. rapa GI* alleles each fully rescued the delayed flowering of *Arabidopsis gi-201* but showed differential rescue of perturbations in red light inhibition of hypocotyl elongation and altered cold and salt tolerance. The *B. rapa* R500 *GI* allele, which failed to rescue the hypocotyl and abiotic stress phenotypes, disrupted circadian period determination in *Arabidopsis*. Analysis of chimeric *B. rapa GI* alleles identified the causal nucleotide polymorphism, which results in an amino acid substitution (S264A) between the two GI proteins. This polymorphism underlies variation in circadian period, cold and salt tolerance, and red light inhibition of hypocotyl elongation. Loss-of-function mutations of *B. rapa GI* confer delayed flowering, perturbed circadian rhythms in leaf movement, and increased freezing and increased salt tolerance, consistent with effects of similar mutations in *Arabidopsis*. Collectively, these data suggest that allelic variation of *GI*—and possibly of clock genes in general—offers an attractive target for molecular breeding for enhanced stress tolerance and potentially for improved crop yield.**

abiotic stress tolerance | circadian clock | hypocotyl elongation | flowering time | natural variation

The last half-century has seen dramatic increases in agricultural productivity. Despite the approximate doubling in world population since 1964, the proportion with insufficient food has dropped by ∼75%, although ∼1 billion remain underfed, and twice that many suffer from micronutrient deficiencies (1). Predicted growth in population and in per capita consumption will require an estimated doubling of crop production by 2050 (2). However, yield trends for maize, rice, wheat, and soybean—four major crops that currently produce nearly two-thirds of global agricultural calories—are insufficient to achieve this doubling (3). Therefore, there is a pressing need not simply to sustain, but actually to accelerate yield improvement.

One strategy to increase yield is to identify genetic variation in plant regulatory networks that limit yield to define targets for programs of marker-assisted (molecular) breeding. The circadian clock has been implicated as a target for increasing yield (4–6). Plant circadian clocks comprise multiple interlocked feedback loops (7–9). There is natural variation in clock function in both weedy and cultivated species (10–15), although few of the genes responsible for these quantitative trait loci (QTL) have been identified. We identified QTL for circadian period in a population of Recombinant Inbred Lines (RIL) of *Brassica rapa* (14). Here we identify *GIGANTEA* (*GI*) as a major QTL responsible for natural variation in circadian period and identify the causal nucleotide polymorphism. We further show that this same nucleotide polymorphism underlies variation in cold and salt tolerance. We suggest that allelic variation of GI—and possibly of clock genes in general—offers a tractable route for molecular breeding for enhanced stress tolerance and potentially for improved crop yield.

Results

B. rapa QTL for circadian period length were identified in a RIL population developed from a cross between the oilseed R500 and the rapid cycling IMB211 (14). We exploited the reference genomic sequence of *B. rapa* (16) to develop additional DNA markers to refine the map position of a period QTL, *PERIODA9a* (*PERA9a*), detected on chromosome A9 (Fig. 1 *A* and *B*) to a position between two genes, *Bra024534* and *Bra024560* (Fig. 1*C*), and spanned by BAC B020D15 (17). Among the 27 genes in that chromosomal region, *GI* (*Bra024536*) was a particularly strong candidate to explain *PERA9a* (Fig. 1*C*) because *GI* affects circadian clock function in *Arabidopsis* (18–21).

Significance

The plant circadian clock affects many aspects of growth and development and influences both fitness in natural settings and performance in cultivated conditions. We show that *GIGANTEA* (*GI*) underlies a major quantitative trait locus for circadian period in *Brassica rapa* by fine-mapping, analysis of heterogeneous inbred lines, and transgenic rescue of an *Arabidopsis gi-201* loss-of-function mutant. Analysis of chimeric and mutated *B. rapa GI* alleles identified the causal nucleotide polymorphism responsible for the allelic variation in circadian period, cold and salt tolerance, and red light inhibition of hypocotyl elongation. Allelic variation of *GI* and of clock genes in general offers targets for marker-assisted (molecular) breeding for enhanced stress tolerance and potentially for improved crop yield.

Author contributions: Q.X., P.L., V.H., D.-J.Y., W.Y.K., B.E.E., C.W., and C.R.M. designed research; Q.X., P.L., V.H., R.A., H.J.P., M.J.S., S.L.K., and D.L.P.S. performed research; Q.X., P.L., V.H., R.A., H.J.P., D.-J.Y., W.Y.K., M.J.S., B.E.E., C.W., and C.R.M. analyzed data; and Q.X., P.L., V.H., D.-J.Y., W.Y.K., B.E.E., C.W., and C.R.M. wrote the paper.

The authors declare no conflict of interest.

This article is a PNAS Direct Submission.

[1]Q.X. and P.L. contributed equally to this work.

[2]To whom correspondence should be addressed. Email: c.robertson.mcclung@dartmouth.edu.

This article contains supporting information online at www.pnas.org/lookup/suppl/doi:10.1073/pnas.1421803112/-/DCSupplemental.

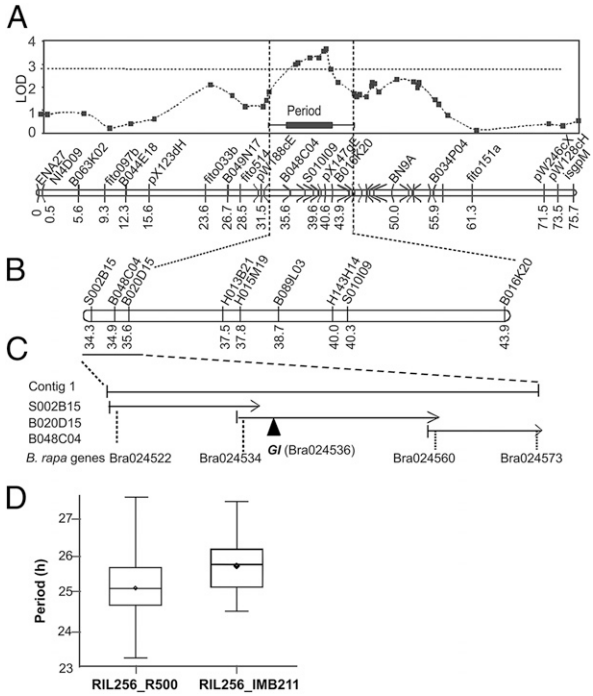

Fig. 1. Fine mapping and genetic definition of the PERA9a circadian period QTL. (*A*) Circadian period QTL on chromosome 9 (PERA9a), redefined by composite interval mapping using the data of Lou et al. (14). (*B*) Fine mapping of the PERA9a QTL using new molecular markers flanking the QTL. (*C*) Three overlapping BAC clones (17) spanning the PERA9a QTL with molecular markers used for fine mapping. (*D*) Period analysis of HIL RIL256_R500 homozygous for R500 and RIL256_IMB211 homozygous for IMB211 in the region of the PERA9a QTL. Box plots show median with the bottom and top of the box indicating 25% and 75%, respectively; whiskers indicate the maximum and minimum values.

PERA9a was detected both at 12° and at 25 °C and at each temperature explained ∼10% of the variation in period length (14). To confirm the presence of *PERA9a* by genetic means, we took advantage of residual heterozygosity in the *GI* region of chromosome A9 in RIL256 (Fig. S1). We allowed RIL256 to self-fertilize and identified lines homozygous for IMB211 (RIL256_IMB211) or for R500 (RIL256_R500) in the *GI* region of A9 in an otherwise uniform genetic background. An additional recombination during the development of RIL256_R500 reduced the region of R500 DNA to ∼10 cM covering the *PERA9a* QTL (Fig. S1*A*). The period of RIL256_R500 was significantly shorter than that of RIL256_IMB211 (Fig. 1*D* and Table S1), which is consistent with the effects of the QTL (14).

If *GI* were indeed the gene responsible for the *PERA9a* QTL, it should be polymorphic in either sequence or expression level between the RIL parents. We detected many single nucleotide polymorphisms (SNPs) in the transcribed portions of the two parental *GI* alleles (Fig. 2*A*). Most SNPs were predicted to be functionally silent, either falling in introns or failing to change the predicted amino acid sequence. However, three SNPs at nucleotide positions 1,274; 2,268; and 2,475 (numbered relative to the A of the initiator AUG in a multiple sequence alignment) were predicted to result in the amino acid polymorphisms S264A, I541T, and D610V, respectively, where the amino acid found in IMB211 is listed before and that found in R500 is listed after the amino acid number. To test the functionality of the two alleles, we performed transgenic rescue experiments in the *Arabidopsis gi-201* loss-of-function background, introducing full genomic copies of each *B. rapa GI* allele driven by their endogenous promoters. In our hands at 22 °C, *gi-201* does not affect circadian period (Fig. 2*B*, Fig. S2, and Table S1), consistent with earlier observations with *gi-2*, another strong loss-of-function allele (22). *gi-201* mutants are late flowering (Fig. 3*A* and Fig. S3*A*) and exhibit a long hypocotyl in red and blue light (Fig. 3*B* and Fig. S3*B*). Both the IMB211 ($BrGI^{IMB211}$) and R500 ($BrGI^{R500}$) *GI* alleles fully rescued the late flowering defect of *Arabidopsis gi-201* (Fig. 3*A* and Fig. S3*A*), indicating that both alleles are expressed and functional, at least for flowering time. In contrast, $BrGI^{IMB211}$, but not $BrGI^{R500}$, fully rescued the long hypocotyl in red light (Fig. 3*B*), indicating that $BrGI^{R500}$ is defective in this trait. Both $BrGI^{IMB211}$ and $BrGI^{R500}$ rescued the long hypocotyl in blue light (Fig. S3*B*), although the rescue by $BrGI^{R500}$ was only partial, suggesting that it is partially but not fully functional for this trait. $BrGI^{IMB211}$ had no effect on circadian period of *gi-201* but, strikingly, introduction of $BrGI^{R500}$ resulted in a significant period shortening (Fig. 2*B*, Fig. S2*A*, and Table S1), consistent with the shorter period of R500 relative to IMB211. Both *BrGI* alleles show similar expression patterns in the *B. rapa* RIL parents (Fig. S4*A*) and in *Arabidopsis gi-201* (Fig. S4*B*), indicating that the differential effect on circadian period does not result from differential expression of the two alleles.

As noted above, three SNPs were predicted to change the amino acid sequence of the GI protein. To determine whether one or more of those changes was responsible for the functional differences between the two alleles, we constructed chimeric alleles, $BrGI^{IMB211(R500)}$ and $BrGI^{R500(IMB211)}$, in which a SacI–NdeI restriction fragment containing four SNPs at nucleotides 1,210; 1,213; 1,274; and 1,295 (Fig. 2*A*) was exchanged.

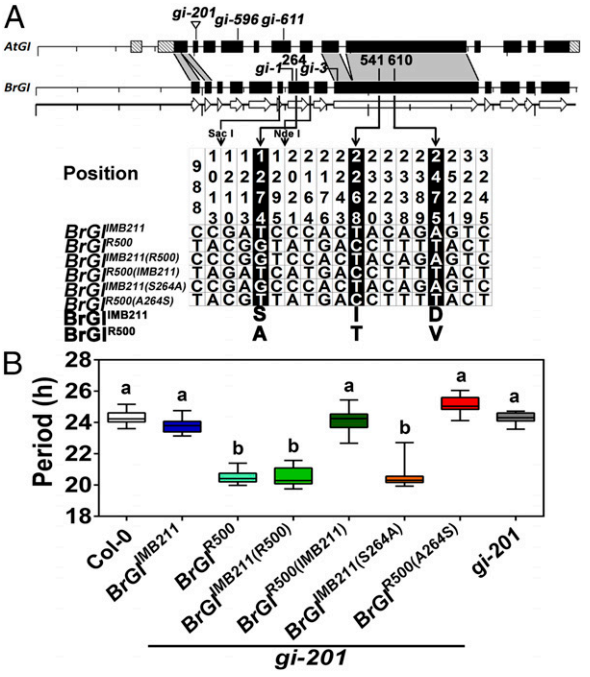

Fig. 2. Transgenic complementation confirms *GI* as the gene underlying the PERA9a QTL. (*A*) Cartoon of the *Arabidopsis* and *B. rapa GI* genes with exons represented by boxes (coding regions in black). Known *gi* mutations are indicated. The numbers 264, 541, and 610 indicate amino acid polymorphisms detailed in *Lower*. *Lower* indicates the nucleotide and amino acid polymorphisms between the *R500*, *IMB211*, and chimeric *GI* alleles. (*B*) Circadian period of *Arabidopsis* Col-0 and *gi-201* lines and of *gi-201* lines carrying the indicated *B. rapa GI* alleles. Box plots show median, with the bottom and top of the box indicating 25% and 75%, respectively; whiskers indicate maximum and minimum values. Different letters indicate values that are statistically different as determined by ANOVA followed by Tukey's test (Table S1).

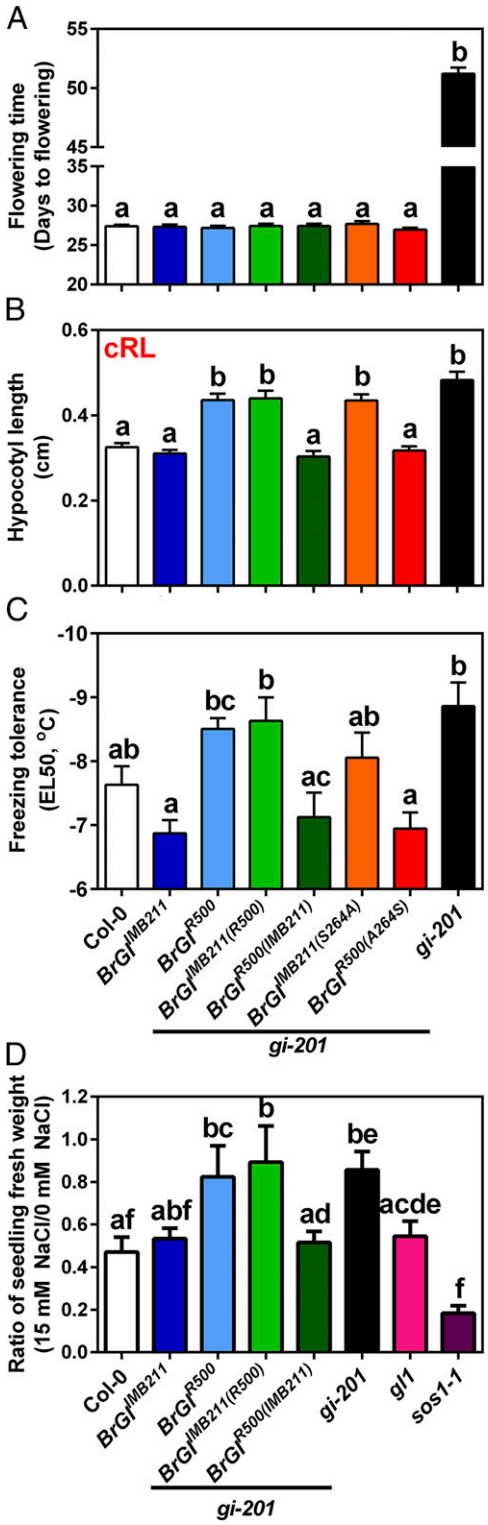

Fig. 3. Transgenic complementation analysis of the role of *GI* in flowering time, photomorphogenesis, cold tolerance, and salt tolerance. *Arabidopsis* Col-0 and *gi-201* and *gi-201* lines carrying the indicated *B. rapa GI* alleles were measured for flowering time, as measured by days to flowering (*A*); photomorphogenesis, as indicated by hypocotyl length in continuous red light (cRL) (*B*); freezing tolerance, expressed as EL50, the temperature at which 50% of leaf electrolytes are lost (*C*); and salt tolerance, measured as fresh weight of total aerial tissues after growth on 1/2 strength MS medium containing 15 mM NaCl relative to growth without NaCl (*D*). All data are presented as mean ± SEM. Different letters indicate values that are statistically different as determined by ANOVA followed by Tukey's test (Table S1).

When tested in transgenic plants, $BrGI^{R500}$ shortened period, but $BrGI^{R500(IMB211)}$ did not (Fig. 2*B*, Fig. S2 *A* and *B*, and Table S1). Conversely, although $BrGI^{IMB211}$ did not shorten period, $BrGI^{IMB211(R500)}$ shortened period to the same extent as $BrGI^{R500}$ (Fig. 2*B*, Fig. S2 *A* and *B*, and Table S1). Thus, we conclude that the differential effects of these two alleles on period length are conferred by the polymorphisms in this SacI–NdeI restriction fragment. Of the four SNPs in this region, only the one at nucleotide 1,274 was predicted to change the amino acid sequence. We therefore used site-directed mutagenesis to make two new *GI* alleles, $BrGI^{IMB211(S264A)}$ in which nucleotide 1,274 of $BrGI^{IMB211}$ was changed from T to G, changing amino acid 264 from S to A, and $BrGI^{R500(A264S)}$ in which nucleotide 1,274 of $BrGI^{R500}$ was changed from G to T, changing amino acid 264 from A to S. These alleles were introduced into *Arabidopsis gi-201*. Although $BrGI^{R500}$ shortened period, $BrGI^{R500(A264S)}$ did not (Fig. 2*B*, Fig. S2 *A* and *C* and Table S1). Conversely, although $BrGI^{IMB211}$ did not shorten period, $BrGI^{IMB211(S264A)}$ shortened period to the same extent as $BrGI^{R500}$ (Fig. 2*B*, Fig. S2 *A* and *C*, and Table S1). All of the *BrGI* alleles were similarly expressed in *Arabidopsis gi-201* seedlings (Fig. S4 *B* and *C*), indicating that the different effects on circadian period do not result from differential expression of the transgenes. Thus, we conclude that the polymorphism at nucleotide 1,274 (T1274G, encoding S264A, with the IMB211 allele listed first) is responsible for the differential effects of these two alleles on period length and that it is the presence of R500 information at nucleotide 1,274, encoding an A residue, that shortens period.

We also tested the phenotypic consequences of introduction of these chimeric and point mutant *BrGI* alleles on flowering time and hypocotyl length. All six *BrGI* alleles rescued the late flowering time of *Arabidopsis gi-201* equally (Fig. 3*A* and Fig. S3*A*). As indicated above, $BrGI^{IMB211}$, but not $BrGI^{R500}$, rescued the long hypocotyl in red light (Fig. 3*B*). Both $BrGI^{R500(IMB211)}$ and $BrGI^{R500(A264S)}$, but neither $BrGI^{IMB211(R500)}$ nor $BrGI^{IMB211(S26S4A)}$, rescued the long hypocotyl in red light (Fig. 3*B*). In blue light, a similar pattern was observed, although in this case $BrGI^{R500}$, $BrGI^{IMB211(R500)}$, and $BrGI^{IMB211(S26S4A)}$ retained partial function and partially but not fully rescued the long hypocotyl phenotype of *gi-201* (Fig. S3*B*). Thus, we conclude that the polymorphism at nucleotide 1,274 is responsible for the differential effects of these alleles on hypocotyl length, and the presence of IMB211 information at nucleotide 1,274 is necessary to fully rescue the long hypocotyl in blue and red light phenotypes of *gi-201*.

Our transgenic rescue experiments established the importance of *BrGI* in circadian period and flowering time determination in *Arabidopsis*. To test whether *GI* functions similarly in *B. rapa*, we identified a set of TILLING mutations in *B. rapa* R-*o*-18, which is closely related to R500 (23). Two putative null alleles, *gi-1* and *gi-3*, were predicted to be strong loss-of-function alleles due to missense mutations (*gi-1*, G1223A; W258Stop and *gi-3*, G1737A; W375Stop) and were analyzed after two back-crosses to the R-*o*-18 parent. *B. rapa* lines homozygous for either *gi-1* or *-3* flower late (Fig. 4 *A* and *B*), consistent with loss of GI function. Circadian period was unaffected at 18 °C (Fig. 4 *C*–*E*), but at 22 °C, most seedlings were arrhythmic, and those that showed circadian rhythms in leaf movement (31% of *B. rapa gi-1* and 42% of *gi-3* mutant seedlings) showed long period and increased relative amplitude error (RAE), a measure of the strength of a circadian rhythm (Fig. 4*E* and Table S1). Thus, mutational disruption of *GI* weakens rhythms in *B. rapa* leaf movement at high temperature. This finding is consistent with *Arabidopsis*, where *GI* plays a critical role in maintaining rhythmicity in leaf movement at higher temperatures (24). However, the role of *GI* in rhythmicity may not be limited to high temperature. In *Arabidopsis*, *GI* is important for maintenance of rhythmicity of *CAB2:LUC* expression at both high and low temperatures (24).

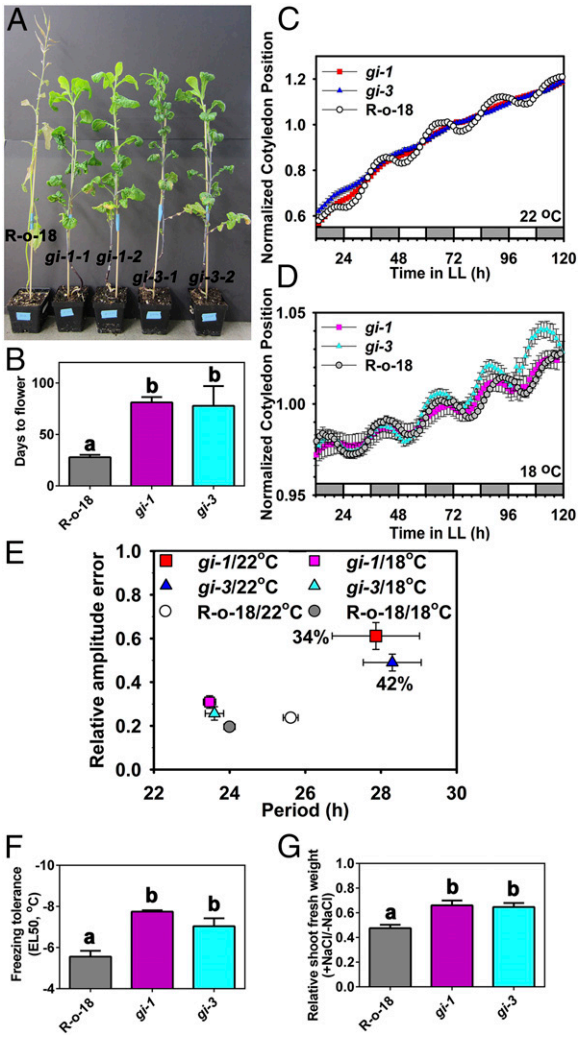

Fig. 4. Characterization of *B. rapa* loss-of-function *gi* alleles. Putative loss-of-function *gi* alleles were identified by TILLING in *B. rapa* R-o-18 (23), which is closely related to R500. (*A*) Images of *gi-1* and *-3* relative to wild-type R-o-18 taken as R-o-18 seeds are drying. (*B*) Quantification of flowering time in *gi-1* and *-3* relative to wild-type R-o-18 expressed as days to first flower. (*C* and *D*) Circadian pattern of cotyledon movement in *B. rapa* R-o-18, *gi-1*, and *gi-3* at 22 °C (*C*) and 18 °C (*D*). (*E*) Quantification of circadian period of R-o-18, *gi-1*, and *gi-3* (mean ± SEM; $n = 12–35$) plotted vs. relative amplitude error (RAE), a measure of the strength of a circadian rhythm. An ideal cosine wave is defined as RAE = 0, and RAE = 1 defines the statistically detectable limit of rhythmicity (53). (*F*) Effect of loss-of-function *GI* mutations on freezing tolerance, expressed as EL50 (the temperature at which 50% of leaf electrolytes are lost) compared with isogenic wild-type *B. rapa* R-o-18. (*G*) Effect of loss-of-function *GI* mutations on salt tolerance compared with isogenic wild-type *B. rapa* R-o-18. Data are presented as the mean ± SEM of shoot fresh weight of seedlings ($n > 35$) grown with 200 mM NaCl/average shoot fresh weight of seedlings grown without NaCl. (*B*, *F*, and *G*) Different letters indicate values that are statistically different as determined by ANOVA followed by Tukey's test (Table S1).

Recently, *GI* has been implicated in cold (25), oxidative (26), drought (27), and salt (28) stress tolerance. Accordingly, we tested our panel of *Arabidopsis gi-201* mutants carrying the *B. rapa GI* alleles for freezing tolerance, as measured by electrolyte leakage after exposure to freezing temperatures. *gi-201* showed significantly greater freezing tolerance than Col-0 (Fig. 3*C*). Transformation of *gi-201* with $BrGI^{R500}$ or with either of the two $BrGI^{IMB211}$ alleles carrying R500 information at nucleotide 1,274 ($BrGI^{IMB211(R500)}$ or $BrGI^{IMB211(S264A)}$) had no effect on freezing tolerance (Fig. 3*C*). However, transformation of *gi-201* with $BrGI^{IMB211}$ or with either of the two $BrGI^{R500}$ alleles carrying IMB211 information at nucleotide 1,274 ($BrGI^{R500(IMB211)}$ or $BrGI^{R500(A264S)}$) significantly reduced freezing tolerance, rescuing the *gi-201* phenotype of increased freezing tolerance (Fig. 3*C*). Thus, we conclude that *B. rapa* GI plays a role in freezing tolerance and that the $BrGI^{IMB211}$ allele is functional in this role, whereas the $BrGI^{R500}$ allele has at least partially lost this function, as has the *Arabidopsis gi-201* allele. To confirm that *GI* also serves as a determinant of freezing tolerance in *B. rapa*, we tested *B. rapa gi-1* and *-3* mutants and found that loss of *GI* function enhanced freezing tolerance, compared with the cognate wild type, R-*o*-18 (Fig. 4*F*).

Our data also suggest a role for GI in nitrogen accumulation. *gi-201* accumulates less N than does Col-0 (Fig. S3*C*). $BrGI^{IMB211}$ and $BrGI^{R500(IMB211)}$ rescue the N content of *gi-201*, but $BrGI^{R500}$ and $BrGI^{IMB211(R500)}$ do not. This finding suggests that IMB211 information at nucleotide 1,274 is necessary for this rescue. However, both point mutants ($BrGI^{IMB211(S264A)}$ and $BrGI^{R500(A264S)}$) rescue the N content of *gi-201*, which is inconsistent with the difference between the two alleles being solely attributable to that single position. Thus, regulation of leaf N content by allelic state at *GI* is not strongly supported by our data; further investigation will be required to resolve the discrepancy among rescue lines.

In contrast, we found no difference among our panel of *Arabidopsis gi-201* mutants carrying the *B. rapa GI* alleles for delta C 13 (Fig. S3*D*) and rosette size (Fig. S3*E*). Thus, these alleles of *GI* do not affect water use efficiency or plant size.

In *Arabidopsis*, *GI* has been shown to function as a negative regulator of resistance to salt stress, and *gi* loss-of-function mutants show increased salt resistance (28). Accordingly, we tested our panel of *Arabidopsis gi-201* mutants carrying the *B. rapa GI* alleles for salt tolerance as measured by fresh weight of aerial tissues following growth in the presence or absence of NaCl. Growth of wild-type Col-0 seedlings or of *glabrous-1* (*gl-1*) was reduced by ∼1/3 at 15 mM NaCl, but *gi-201* was unaffected. Transformation of *gi-201* with $BrGI^{R500}$ or with $BrGI^{IMB211(R500)}$ had no effect on the increased salt tolerance of *gi-201* (Fig. 3*D* and Fig. S5). However, transformation of *gi-201* with $BrGI^{IMB211}$ or with $BrGI^{R500(IMB211)}$ significantly reduced salt tolerance, rescuing the *gi-201* phenotype of increased salt tolerance (Fig. 3*D* and Fig. S5). Thus, we conclude that *B. rapa* GI plays a role in salt tolerance and that the $BrGI^{IMB211}$ allele is fully functional in this role, whereas the $BrGI^{R500}$ allele is impaired in this function, as is the *Arabidopsis gi-201* allele. To confirm that *GI* also serves as a determinant of resistance to salt stress in *B. rapa*, we tested *B. rapa gi-1* and *-3* mutants and found that loss of *GI* function enhanced salt stress resistance compared with the cognate wild type, R-*o*-18 (Fig. 4*G*).

Discussion

GI was first identified as a supervital mutant of *Arabidopsis* (29), with a prolonged phase of vegetative growth that increased reproductive capacity (30, 31). *GI*, in addition to this role in photoperiodic flowering, also is required for phytochrome signaling (20, 32, 33) and for proper clock function (18, 19), although the roles of *GI* in photoperiodic flowering, photomorphogenesis, and the clock can be dissociated (20, 33, 34).

Our results with the *B. rapa GI* alleles extend conclusions drawn from *Arabidopsis* to *Brassica*. Both $BrGI^{R500}$ and $BrGI^{IMB211}$ fully rescue the photoperiodic flowering defect of *Arabidopsis gi-201* mutants. *gi-201* is a strong loss-of-function allele, and full rescue of the *gi-201* late-flowering phenotype demonstrates that both *Brassica* alleles are equally functional in terms of flowering time in *Arabidopsis*. However, the two *B. rapa GI* alleles are not equally functional in terms of hypocotyl elongation, freezing tolerance, and salt tolerance. In each case, $BrGI^{IMB211}$ fully rescued the *gi-201* phenotype, whereas $BrGI^{R500}$

failed to rescue. Thus, the flowering timing function is distinct from the hypocotyl elongation, freezing tolerance, and salt tolerance functions. Amino acid 264 (A in R500 vs. S in IMB211) is therefore important for these latter three functions. Amino acid 264 is also important for circadian period determination, because introduction of $BrGI^{R500}$ (and $BrGI^{IMB211}$ alleles carrying R500 information at amino acid 264), but not $BrGI^{IMB211}$ (and $BrGI^{R500}$ alleles carrying IMB211 information at amino acid 264), shortens circadian period.

GI functions typically involve protein–protein interactions. For example, in flowering timing, GI interacts with the F-box protein FLAVIN BINDING KELCH REPEAT F-BOX PROTEIN1 (FKF1), and in the afternoon this GI–FKF1 complex degrades CYCLING DOF FACTORS (CDFs) bound at the *CONSTANS* (*CO*) promoter, relieving transcriptional repression and allowing the accumulation of *CO* mRNA in the light (35, 36). CO protein is stabilized in the light, accumulates, and induces expression of *FT*, which induces floral identity genes. GI also binds to the *FT* promoter and interacts directly with the *FT* repressors, SHORT VEGETATIVE PHASE (SVP), TEMPRANILLO 1 (TEM1), and TEM2, to directly induce *FT* (37). Relevant to the nuclear roles of GI in the regulation of *CO* and *FT* expression is a protein–protein interaction with ELF4 that confers subnuclear localization and restricts chromatin access of GI (38). Finally, GI protein stability is controlled by interaction with EARLY FLOWERING3 (ELF3) and the E3 ubiquitin ligase CONSTITUTIVELY PHOTOMORPHOGENIC1 (COP1) (39). At least some of these functions are retained in *B. rapa*, because *B. rapa gi* loss-of-function mutants are late flowering. Both *BrGI* alleles fully rescue the flowering delay of *Arabidopsis gi-201*, suggesting that both BrGI proteins retain all these interactions.

In its role in circadian period determination, in the light GI binds to and stabilizes ZEITLUPE (ZTL), an F-box protein closely related to FKF1. The conformational shift in ZTL that follows the cessation of blue light signaling after dusk releases GI, freeing ZTL to interact with and thereby target critical clock transcriptional repressors, TOC1 and PRR5, for ubiquitylation and proteasomal degradation (40, 41). Because ZTL is a cytoplasmic protein, the ZTL–GI interaction also retains GI in the cytosol, thereby limiting the nuclear accumulation of GI and antagonizing its roles in flowering timing and regulation of hypocotyl length (42).

The effects on circadian period of $BrGI^{R500}$ and $BrGI^{IMB211}$ and their derivatives when transformed into *Arabidopsis gi-201* demonstrate an important role for amino acid 264 in circadian period definition. First, we note that $BrGI^{R500}$ shortens circadian period length and acts as a gain-of-function mutant relative to $BrGI^{IMB211}$. The amino acid change of S264 in $BrGI^{IMB211}$ to A in $BrGI^{R500}$ is similar to that observed in the *Arabidopsis gi-200* short period allele (S932A) (20), although the two mutations lie in different regions of the coding sequence. Moreover, the *Arabidopsis* Col-0 amino acid at the position corresponding to *B. rapa GI* 264 is A, and this residue is conserved in four *Arabidopsis* accessions, barley and wheat (12). This finding suggests that the phenotypic consequences of differing information at amino acid 264 cannot be determined solely by the amino acid at that residue but, rather, must be considered in the context of the entire protein sequence.

One possible molecular explanation of the effect of the $BrGI^{R500}$ phenotype of short period could be an increased affinity of $BrGI^{R500}$ for ZTL, which would stabilize ZTL, increase ZTL accumulation, and thereby shorten period (43). This explanation would be consistent with the observed effects on red light inhibition of hypocotyl elongation, because the increased affinity of $BrGI^{R500}$ for ZTL would limit nuclear accumulation and thereby antagonize the ability of $BrGI^{R500}$ to rescue red light inhibition of hypocotyl elongation. However, both *B. rapa GI* alleles fully rescue the flowering timing phenotype of *gi-201*. Therefore, if differential affinities for ZTL explain the period differences of the *B. rapa GI* alleles, these effects must not limit nuclear accumulation of GI to the point where flowering timing is compromised.

The role of GI in red and blue light suppression of hypocotyl elongation is incompletely defined. GI has been suggested to regulate CRY-mediated blue light signaling (44). The long hypocotyl in red light phenotype of *gi-2* is suppressed in *spindly-4* (*spy-4*) *gi-2* double mutants, and, consistent with this genetically defined interaction, SPY and GI proteins interact (22).

More recently, GI has emerged as a key player in a number of stress responses, notably to drought, cold, and salinity (25, 27, 28). Loss of GI function in *Arabidopsis* results in increased tolerance to both freezing and salt stress in *Arabidopsis*, and our analysis of *B. rapa GI* loss-of-function mutants shows a similar enhancement of freezing and salt resistance in *B. rapa*, suggesting that the roles of GI in resistance to these two stresses is conserved between species. Among these stresses, the role of GI in salt tolerance is best understood. In *Arabidopsis*, GI sequesters SALT OVERLY SENSITIVE2 (SOS2), a protein kinase that serves as a positive regulator of salt tolerance (28). Release of SOS2 from GI in response to elevated salt permits formation of the SOS2/SOS3 protein kinase complex that associates with and phosphorylates SOS1, activating its Na^+/H^+ antiport activity and enhancing salt tolerance (45). Differential rescue of the salt tolerance phenotype of *Arabidopsis gi-201* by $BrGI^{IMB211}$ and $BrGI^{R500}$allows the prediction of the *Arabidopsis* model is that $BrGI^{IMB211}$ has greater affinity for SOS2 than does $BrGI^{R500}$.

It is important to note that most of our experiments tested the function of *BrGI* alleles in *Arabidopsis*. Extrapolating the complex network of GI functions elucidated in *Arabidopsis* into *B. rapa* and determining the mechanistic basis of the functional differences observed between the two *BrGI* alleles will likely be complicated by the triplication of the *B. rapa* genome since its separation from *Arabidopsis* (46). In the *B. rapa* reference Chiifu genome, subsequent gene loss has eliminated two of the duplicated *GI* copies, leaving a single *GI* locus (47). Similarly, there are single copies of *SOS2* and of *TEM2* (47). However, other potential GI interactors are present in two (*CDF1*, *CDF2*, *CDF3*, *COP1*, *ELF3*, *FT*, *SPY*, *SVP*, and *TEM1*) or three (*ELF4*) copies (47), and some or all of these copies have likely diverged from their *Arabidopsis* homologs as well as from each other through subfunctionalization. Of interest in the context of circadian period determination, *B. rapa* has lost all copies of both *ZTL* and *FKF1* (48). In *B. rapa*, the functions of *ZTL* and *FKF1* are presumably carried out by a third family member, *LOV KELCH PROTEIN2* (*LKP2*), which exhibits partial functional redundancy with *ZTL* and *FKF1* in *Arabidopsis* (49). In *B. rapa*, *LKP2* is present in three linked copies resulting from a complex tandem gene triplication (48). It will be of interest to determine whether subfunctionalization among these three copies of *LKP2* has resulted in the specialization of one or more copies for flowering timing or circadian functions.

Materials and Methods

Plant Materials. All constructs were transformed by floral dip into the *Arabidopsis gi-201* mutant (20) carrying the *proCCA1:LUC* transgene (50). Seeds were sterilized in 20% (vol/vol) bleach and placed on half-strength Murashige and Skoog (MS) medium with 0.8% agar and 2% (wt/vol) sucrose, then stratified for 3 d at 4 °C in the dark.

Fine Mapping the *GI* QTL. To confirm the circadian period QTL on chromosome 9, simple sequence repeat (SSR) markers were developed based on sequenced BAC clones (17). In total, 13 SSR markers were used to fine-map the A9 QTL region (Table S2). Heterogeneous inbred lines (HILs) were generated from an F4 RIL, RIL256, heterozygous in the A9 QTL region. We then genotyped 144 plants of the F5 generation of RIL256 using our SSR markers to identify HILs of RIL256 homozygous for either IMB211 (RIL256_IMB211) or R500 (RIL256_R500) in the QTL region.

Constructs. PCR products of full-length $BrGI^{R500}$ and $BrGI^{IMB211}$ genomic DNA, including promoters and 3′ UTR, were amplified from genomic DNA with primer pairs Br_GI_locus_F1 and Br_GI_locus_R1 by using Phusion High-Fidelity DNA Polymerase (New England Biolabs) and cloned into pENTR. SacI and NdeI were used to make chimeric genes, $BrGI^{IMB211(R500)}$ and $BrGI^{R500(IMB211)}$, in which the fragments that included the first different amino acid (S264A) were switched between $BrGI^{IMB211}$ and $BrGI^{R500}$, respectively. Three primers, I-S1F2, RI-S1R2, and R-S1F2, were used to make site-specific mutation constructs, $BrGI^{IMB211(S264A)}$ and $BrGI^{R500(A264S)}$. All pENTR_GI constructs were recombined into binary vector pH2GW7Δ (51).

Phenotypic Analysis. For circadian period determination, seedlings were entrained in 12-h light/12-h dark LD cycles under white light (70 $\mu mol \cdot m^{2} \cdot s^{-1}$) at 22 °C before release into continuous light and temperature for LUC activity measurement with a TopCount luminometer (Perkin-Elmer Life Sciences). Circadian period estimation in *B. rapa* lines was by cotyledon movement as described (52). Data analysis was with BRASS (Version 2.1.4), which employs fast Fourier transform nonlinear least squares (53). Details of other phenotypic analyses are provided in *SI Materials and Methods*. Statistical significance for circadian period and other phenotypic analyses was with ANOVA followed by Tukey's test, which performs all pairwise comparisons and corrects for multiple comparisons.

ACKNOWLEDGMENTS. We thank K. Greenham for helpful comments. This work was supported by National Science Foundation Grants IOS-0923752 and IOS-1025965, the National Research Foundation of Korea Grant 2013R1A2A1A01005170, and Rural Development Administration, Republic of Korea Next-Generation BioGreen 21Programme, Systems & Synthetic Agrobiotech Center, Grants PJ01106901 and PJ01106904.

1. Godfray HCJ, et al. (2010) Food security: The challenge of feeding 9 billion people. *Science* 327(5967):812–818.
2. Tilman D, Balzer C, Hill J, Befort BL (2011) Global food demand and the sustainable intensification of agriculture. *Proc Natl Acad Sci USA* 108(50):20260–20264.
3. Ray DK, Mueller ND, West PC, Foley JA (2013) Yield trends are insufficient to double global crop production by 2050. *PLoS ONE* 8(6):e66428.
4. Dodd AN, et al. (2005) Plant circadian clocks increase photosynthesis, growth, survival, and competitive advantage. *Science* 309(5734):630–633.
5. Graf A, Schlereth A, Stitt M, Smith AM (2010) Circadian control of carbohydrate availability for growth in *Arabidopsis* plants at night. *Proc Natl Acad Sci USA* 107(20): 9458–9463.
6. Ng DW-K, et al. (2014) A role for CHH methylation in the parent-of-origin effect on altered circadian rhythms and biomass heterosis in *Arabidopsis* intraspecific hybrids. *Plant Cell* 26(6):2430–2440.
7. McClung CR (2011) The genetics of plant clocks. *Adv Genet* 74:105–139.
8. Hsu PY, Harmer SL (2014) Wheels within wheels: The plant circadian system. *Trends Plant Sci* 19(4):240–249.
9. McClung CR (2014) Wheels within wheels: New transcriptional feedback loops in the Arabidopsis circadian clock. *F1000Prime Rep* 6:2.
10. Michael TP, et al. (2003) Enhanced fitness conferred by naturally occurring variation in the circadian clock. *Science* 302(5647):1049–1053.
11. Edwards KD, et al. (2006) *FLOWERING LOCUS C* mediates natural variation in the high-temperature response of the Arabidopsis circadian clock. *Plant Cell* 18(3): 639–650.
12. Edwards KD, Lynn JR, Gyula P, Nagy F, Millar AJ (2005) Natural allelic variation in the temperature-compensation mechanisms of the *Arabidopsis thaliana* circadian clock. *Genetics* 170(1):387–400.
13. Salathia N, Lynn JR, Millar AJ, King GJ (2007) Detection and resolution of genetic loci affecting circadian period in *Brassica oleracea*. *Theor Appl Genet* 114(4):683–692.
14. Lou P, et al. (2011) Genetic architecture of the circadian clock and flowering time in *Brassica rapa*. *Theor Appl Genet* 123(3):397–409.
15. Anwer MU, et al. (May 27, 2014) Natural variation reveals that intracellular distribution of ELF3 protein is associated with function in the circadian clock. *elife*, 10.7554/eLife.02206#sthash.04mtZBPu.dpuf.
16. Wang X, et al.; *Brassica rapa* Genome Sequencing Project Consortium (2011) The genome of the mesopolyploid crop species *Brassica rapa*. *Nat Genet* 43(10): 1035–1039.
17. Kim H, et al. (2009) Sequenced BAC anchored reference genetic map that reconciles the ten individual chromosomes of *Brassica rapa*. *BMC Genomics* 10:432.
18. Fowler S, et al. (1999) GIGANTEA: A circadian clock-controlled gene that regulates photoperiodic flowering in Arabidopsis and encodes a protein with several possible membrane-spanning domains. *EMBO J* 18(17):4679–4688.
19. Park DH, et al. (1999) Control of circadian rhythms and photoperiodic flowering by the *Arabidopsis GIGANTEA* gene. *Science* 285(5433):1579–1582.
20. Martin-Tryon EL, Kreps JA, Harmer SL (2007) GIGANTEA acts in blue light signaling and has biochemically separable roles in circadian clock and flowering time regulation. *Plant Physiol* 143(1):473–486.
21. Dalchau N, et al. (2011) The circadian oscillator gene *GIGANTEA* mediates a long-term response of the *Arabidopsis thaliana* circadian clock to sucrose. *Proc Natl Acad Sci USA* 108(12):5104–5109.
22. Tseng T-S, Salomé PA, McClung CR, Olszewski NE (2004) SPINDLY and GIGANTEA interact and act in *Arabidopsis thaliana* pathways involved in light responses, flowering, and rhythms in cotyledon movements. *Plant Cell* 16(6):1550–1563.
23. Stephenson P, et al. (2010) A rich TILLING resource for studying gene function in *Brassica rapa*. *BMC Plant Biol* 10:62.
24. Gould PD, et al. (2006) The molecular basis of temperature compensation in the *Arabidopsis* circadian clock. *Plant Cell* 18(5):1177–1187.
25. Cao S, Ye M, Jiang S (2005) Involvement of *GIGANTEA* gene in the regulation of the cold stress response in *Arabidopsis*. *Plant Cell Rep* 24(11):683–690.
26. Cao S, Jiang S, Zhang R (2006) The role of *GIGANTEA* gene in mediating the oxidative stress response and in *Arabidopsis*. *Plant Growth Regul* 48:261–270.
27. Riboni M, Galbiati M, Tonelli C, Conti L (2013) GIGANTEA enables drought escape response via abscisic acid-dependent activation of the florigens and SUPPRESSOR OF OVEREXPRESSION OF CONSTANS. *Plant Physiol* 162(3):1706–1719.
28. Kim W-Y, et al. (2013) Release of SOS2 kinase from sequestration with GIGANTEA determines salt tolerance in *Arabidopsis*. *Nat Commun* 4:1352.
29. Rédei GP (1962) Supervital mutants of *Arabidopsis*. *Genetics* 47(4):443–460.
30. Koornneef M, Hanhart CJ, van der Veen JH (1991) A genetic and physiological analysis of late flowering mutants in *Arabidopsis thaliana*. *Mol Gen Genet* 229(1):57–66.
31. Araki T, Komeda Y (1993) Analysis of the role of the late-flowering locus, *GI*, in the flowering of *Arabidopsis thaliana*. *Plant J* 3:231–239.
32. Huq E, Tepperman JM, Quail PH (2000) GIGANTEA is a nuclear protein involved in phytochrome signaling in *Arabidopsis*. *Proc Natl Acad Sci USA* 97(17):9789–9794.
33. Oliverio KA, et al. (2007) GIGANTEA regulates phytochrome A-mediated photomorphogenesis independently of its role in the circadian clock. *Plant Physiol* 144(1): 495–502.
34. Mizoguchi T, et al. (2005) Distinct roles of *GIGANTEA* in promoting flowering and regulating circadian rhythms in Arabidopsis. *Plant Cell* 17(8):2255–2270.
35. Fornara F, et al. (2009) Arabidopsis DOF transcription factors act redundantly to reduce *CONSTANS* expression and are essential for a photoperiodic flowering response. *Dev Cell* 17(1):75–86.
36. Sawa M, Nusinow DA, Kay SA, Imaizumi T (2007) FKF1 and GIGANTEA complex formation is required for day-length measurement in Arabidopsis. *Science* 318(5848): 261–265.
37. Sawa M, Kay SA (2011) GIGANTEA directly activates Flowering Locus T in *Arabidopsis thaliana*. *Proc Natl Acad Sci USA* 108(28):11698–11703.
38. Kim Y, et al. (2013) ELF4 regulates GIGANTEA chromatin access through subnuclear sequestration. *Cell Reports* 3(3):671–677.
39. Yu J-W, et al. (2008) COP1 and ELF3 control circadian function and photoperiodic flowering by regulating GI stability. *Mol Cell* 32(5):617–630.
40. Más P, Kim W-Y, Somers DE, Kay SA (2003) Targeted degradation of TOC1 by ZTL modulates circadian function in *Arabidopsis thaliana*. *Nature* 426(6966):567–570.
41. Fujiwara S, et al. (2008) Post-translational regulation of the Arabidopsis circadian clock through selective proteolysis and phosphorylation of pseudo-response regulator proteins. *J Biol Chem* 283(34):23073–23083.
42. Kim J, Geng R, Gallenstein RA, Somers DE (2013) The F-box protein ZEITLUPE controls stability and nucleocytoplasmic partitioning of GIGANTEA. *Development* 140(19): 4060–4069.
43. Somers DE, Kim WY, Geng R (2004) The F-box protein ZEITLUPE confers dosage-dependent control on the circadian clock, photomorphogenesis, and flowering time. *Plant Cell* 16(3):769–782.
44. Crepy M, Yanovsky MJ, Casal JJ (2007) Blue rhythms between GIGANTEA and phytochromes. *Plant Signal Behav* 2(6):530–532.
45. Quintero FJ, Ohta M, Shi H, Zhu JK, Pardo JM (2002) Reconstitution in yeast of the *Arabidopsis* SOS signaling pathway for Na+ homeostasis. *Proc Natl Acad Sci USA* 99(13):9061–9066.
46. Town CD, et al. (2006) Comparative genomics of *Brassica oleracea* and *Arabidopsis thaliana* reveal gene loss, fragmentation, and dispersal after polyploidy. *Plant Cell* 18(6):1348–1359.
47. Cheng F, Wu J, Fang L, Wang X (2012) Syntenic gene analysis between *Brassica rapa* and other Brassicaceae species. *Front Plant Sci* 3:198.
48. Lou P, et al. (2012) Preferential retention of circadian clock genes during diploidization following whole genome triplication in *Brassica rapa*. *Plant Cell* 24(6): 2415–2426.
49. Baudry A, et al. (2010) F-box proteins FKF1 and LKP2 act in concert with ZEITLUPE to control Arabidopsis clock progression. *Plant Cell* 22(3):606–622.
50. Salomé PA, Xie Q, McClung CR (2008) Circadian timekeeping during early Arabidopsis development. *Plant Physiol* 147(3):1110–1125.
51. Karimi M, Inzé D, Depicker A (2002) GATEWAY vectors for Agrobacterium-mediated plant transformation. *Trends Plant Sci* 7(5):193–195.
52. Xu X, Xie Q, McClung CR (2010) Robust circadian rhythms of gene expression in *Brassica rapa* tissue culture. *Plant Physiol* 153(2):841–850.
53. Plautz JD, et al. (1997) Quantitative analysis of *Drosophila period* gene transcription in living animals. *J Biol Rhythms* 12(3):204–217.

Supporting Information

Xie et al. 10.1073/pnas.1421803112

SI Materials and Methods

Expression Analysis by Quantitative RT-PCR. Seedlings were entrained for 10 d in photocycles [12-h/12-h light/dark (12/12 LD) cycles]. Samples were collected every 2 h for one diurnal cycle. RNA was extracted by using the Qiagen RNeasy Plant Mini Kit. First-strand cDNA synthesis used 2 μg of total RNA with the SuperScript III first-strand synthesis system (Invitrogen). The cDNA was diluted 10× with water, and 1 μL was used for PCR amplification using a SYBR Premix Ex Taq II (Takara Bio) with gene-specific primers (Table S2). mRNA abundances were calculated by using the comparative C_T method, with *TUB3* (*Arabidopsis* At5g62700 or *B. rapa* Bra018184) as the normalization control. Data are presented as mean ± SEM of three technical replicates from one representative experiment. The experiment was repeated with essentially identical results.

Flowering Time Determination. Days to flowering (defined as the opening of the first flower) and rosette leaf number at flowering were determined with soil-grown plants at 22 °C in 16/8 LD cycles at 100 $\mu mol \cdot m^{-2} \cdot s^{-1}$ white light at 22 °C in a controlled environment growth room.

Hypocotyl Length. Seeds were cold-treated at 4° C for 3 d, sown on 1/2× MS (no sucrose) 0.8% agar plates, and then exposed to continuous white light for 12 h to induce uniform germination. The plates were transferred to continuous blue (470 nm, 4 $\mu mol \cdot m^{-2} \cdot s^{-1}$) or red (670 nm, 40 $\mu mol \cdot m^{-2} \cdot s^{-1}$) light at 22 °C, and hypocotyl length was measured after 7 d.

Freezing Tolerance. Freezing tolerance was measured by electrolyte leakage as described (1). Seedlings were grown in soil at 22 °C in 12/12 LD cycles for 3 wk and then acclimated to cold (4 °C) for 1 wk. For each temperature and genotype, three replicates each consisting of three or four leaves (*Arabidopsis*) or one leaf (*B. rapa*) from three plants were transferred to a programmable cooling bath set to −2 °C. Samples were cooled at a rate of 2 °C per h, taken from the water bath at 2 °C intervals from −4 to −14 °C, and incubated at 4 °C overnight before adding 4 mL of distilled water to each tube. Electrolyte leakage was determined as the ratio of conductivity before and after boiling the samples. EL50, the value at which 50% of the electrolytes had leaked, was calculated with fitted sigmoidal curves (MATLAB; Version 8.0.0.783, MathWorks).

Salt Tolerance. For *Arabidopsis*, seeds sterilized with 70% ethanol/2% bleach and washed three times with distilled water were spotted directly on rock wool in distilled water for 1 wk. After germination, nutrient medium with and without NaCl (15 mM) was provided. Fresh weight of aerial tissues was measured after 2–3 wk of growth. *sos-1* is a hypersensitive control and was compared with its isogenic wild-type *gl1* (2). For *B. rapa*, seeds sterilized with 70% ethanol/10% bleach and washed three times with distilled water were plated in Magenta boxes on 1/2 strength MS medium with or without 200 mM NaCl. After stratification for 4 d at 4 °C in the dark, plants were grown at 22 °C in 12-h light/12-h dark cycles for 7 d, and shoot fresh weight was determined.

Water Use Efficiency. Seed of the six transgenic rescue genotypes as well as wild-type and *gi-201* mutant were planted on moist Sunshine Sungro LP-5 soil (Sungro Horticulture) and cold-stratified (+4 °C) for 4 d. The pots were then moved to growth chambers (PGC-9/2 with Percival Advanced Intellus Environmental Controller; Percival Scientific; 10/14 LD at 24 °C) for 7 wk. Plants were measured for rosette size, and fully expanded leaves were collected, dried at 65 °C for 4 d, and homogenized for isotope and N analyses. Stable isotope analyses (delta 13 C, %N) were performed by using an elemental analyzer (ECS 4010; Costech Analytical Technologies) coupled to a continuous-flow inlet isotope ratio mass spectrometer (CF-IRMS; Delta-plus XP; Thermo Scientific) at the University of Wyoming Stable Isotope Facility. Delta 13 C values were reported in parts per million relative to Vienna Peedee Belemnite. The precision of repeated measurements of laboratory standards was >>0.11‰. Replicate number per genotype varied from 13 to 21. N content is reported as a percentage of leaf mass.

1. Rohde P, Hincha DK, Heyer AG (2004) Heterosis in the freezing tolerance of crosses between two *Arabidopsis thaliana* accessions (Columbia-0 and C24) that show differences in non-acclimated and acclimated freezing tolerance. *Plant J* 38(5):790–799.

2. Wu S-J, Ding L, Zhu J-K (1996) *SOS1*, a genetic locus essential for salt tolerance and potassium acquisition. *Plant Cell* 8(4):617–627.

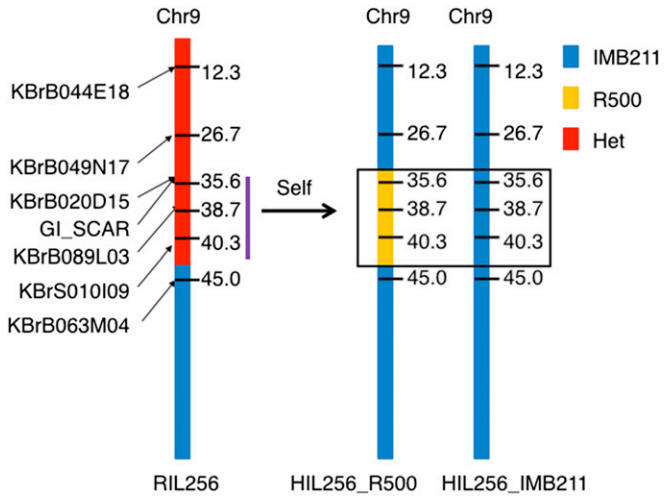

Fig. S1. HILs for genetic confirmation of the PERA9 QTL. Genetic map of chromosome 9 of RIL256, as well as of two HILs in which the heterozygous (Het; shown in red) region surrounding the PERA9a QTL has resolved as R500 (yellow in HIL256_R500) or IMB211 (blue in HIL256_IMB211). Molecular markers for genotyping HIL are at left. Purple line indicates the PERA9a QTL region, and boxed region indicates where the two HIL differ genetically.

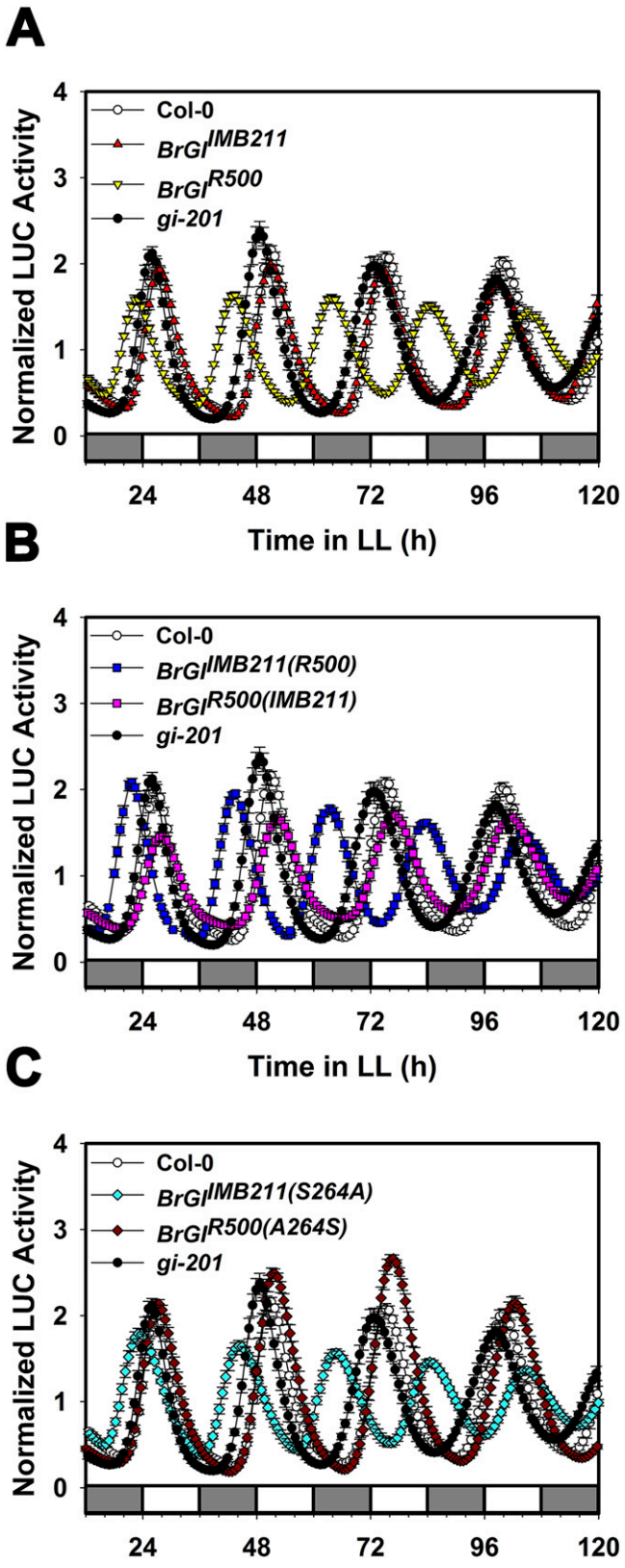

Fig. S2. Effects of *B. rapa GI* alleles on *CCA1:LUC* Expression in *Arabidopsis*. (*A*) *CCA1:LUC* in Col-0 (open circles), *gi-201* (filled circles), and in *gi-201* carrying *B. rapa* GI^{IMB211} (red triangles) and in GI^{R500} (open triangles). (*B*) *CCA1:LUC* in Col-0 (open circles), *gi-201* (filled circles), and in *gi-201* carrying *B. rapa* $GI^{IMB211(R500)}$ (blue squares) and in $GI^{R500(IMB211)}$ (red squares). (*C*) *CCA1:LUC* in Col-0 (open circles), *gi-201* (filled circles), and in *gi-201* carrying *B. rapa* $GI^{IMB211(S264A)}$ (cyan diamonds) and in $GI^{R500(A264S)}$ (dark red diamonds). Seedlings were entrained to photocycles (12/12 LD) at 24 °C for 6 d before release into continuous light (LL) at $T = 0$. Average traces (mean ± SEM, $n = 22–24$) are shown for luciferase (LUC) activity of *CCA1:LUC*, normalized to the average activity over the duration of the experiment. White and gray bars indicate subjective day and night, respectively.

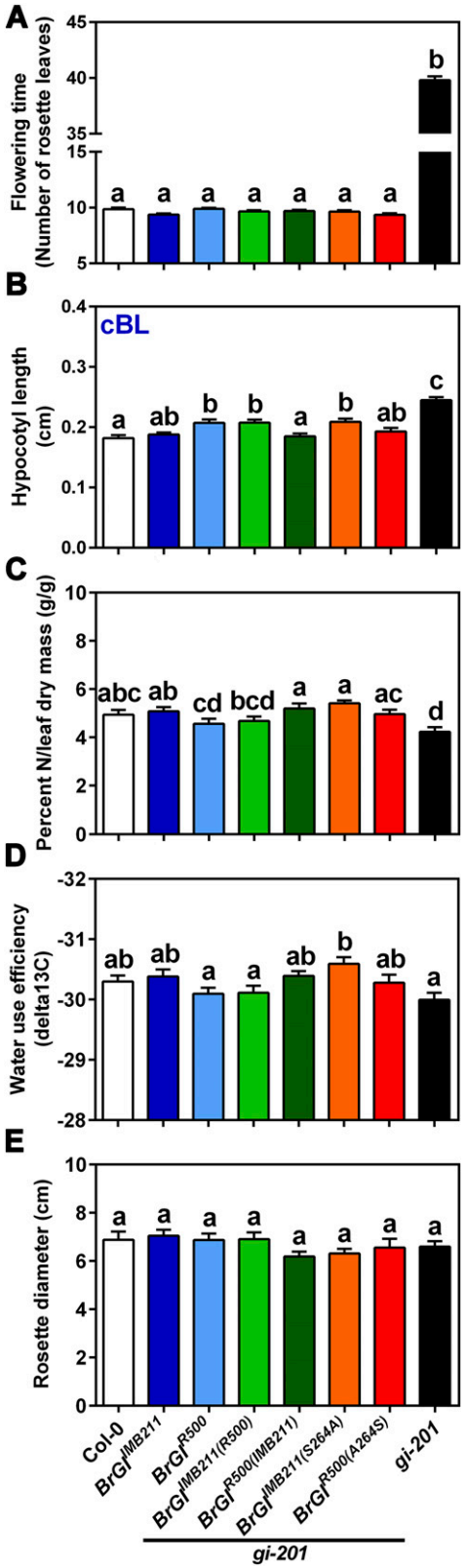

Fig. S3. Transgenic complementation analysis of the role of *GI* in flowering time, photomorphogenesis, water use efficiency, leaf nitrogen content (%N), and rosette size. *Arabidopsis* Col-0 and *gi-201* and *gi-201* lines carrying the indicated *B. rapa GI* alleles were measured for flowering time, as measured by number of rosette leaves at flowering (*A*); photomorphogenesis, as indicated by hypocotyl length in continuous blue light (cBL) (*B*); leaf nitrogen content (%N) (*C*); water use efficiency (delta 13C) (*D*); and rosette diameter (*E*). All data are presented as mean ± SEM. Different letters indicate values that are statistically different as determined by ANOVA followed by Tukey's test (Table S1).

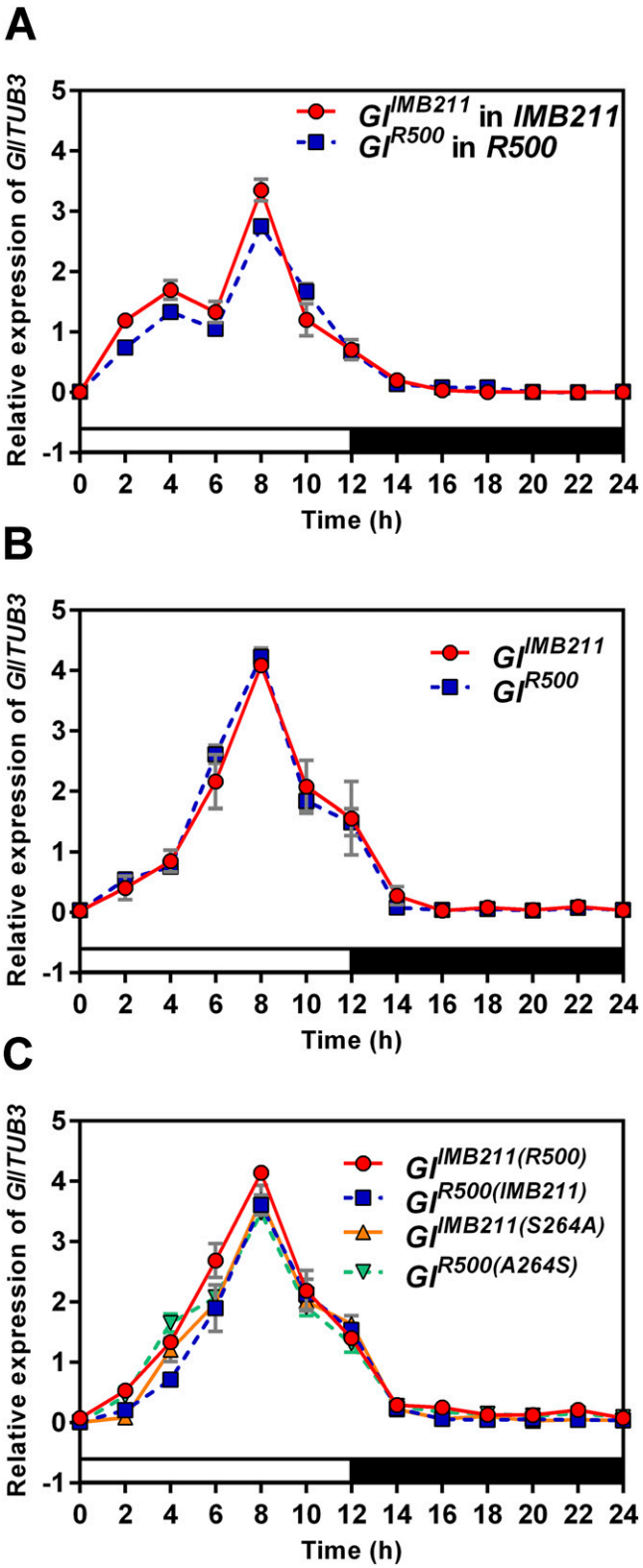

Fig. S4. Expression of the *B. rapa GI* alleles in the *B. rapa* RIL parents and driven from their endogenous promoters in transgenic *Arabidopsis*. *GI* transcript abundance in *B. rapa* IMB211 (red circles) and in R500 (blue squares) (*A*), in *Arabidopsis gi-201* carrying $BrGI^{IMB211}$ (red circles) or $BrGI^{R500}$ (blue squares) (*B*), and in *Arabidopsis gi-201* carrying $BrGI^{IMB211(R500)}$ (red circles), $BrGI^{R500(IMB211)}$ (blue squares), $BrGI^{IMB211(S264A)}$ (orange triangles), or $BrGI^{R500(A264S)}$ (green triangles) (*C*). Total RNA was isolated from seedlings grown in photocycles (LD; 12-h light/12-h dark) at 24 °C and sampled every 2 h over a complete day. Transcript levels were determined by quantitative RT-PCR (qPCR) and normalized to *TUBULIN3c* (*Tub3c*). White and black bars indicate light and dark.

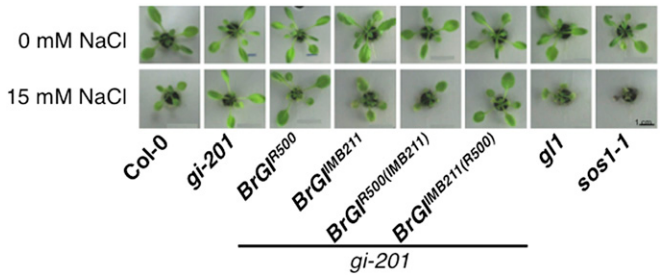

Fig. S5. Effects of *B. rapa GI* alleles on salt tolerance of transgenic *Arabidopsis*. Growth of *Arabidopsis* Col-0, *gi-201*, and of *gi-201* lines carrying the indicated *B. rapa GI* alleles. Seedlings were grown on ½-strength MS medium solidified with 1% agar for 1 wk, and then the medium was amended to 0 or 15 mM NaCl for 1 wk. *Arabidopsis sos1-1* is overly sensitive to salt, as indicated by comparison with its isogenic parent, *Arabidopsis gl-1* (1), and is shown as a control.

1. Wu S-J, Ding L, Zhu J-K (1996) *SOS1*, a genetic locus essential for salt tolerance and potassium acquisition. *Plant Cell* 8(4):617–627.

Table S1. Summary of phenotypic characterization of *GI* mutants and transgenic complementation

	Mean	SEM	*n*	*P*
Circadian period of HILs (Fig. 1*D*)				
RIL256-R500	25.15	0.01	56	—
RIL256-IMB211	25.72	0.043	25	0.004
Circadian period of *Arabidopsis gi-201* transformed with *BrGI* alleles (Fig. 2*B*)				
Col-0	24.31	0.08	23	0.999*
$BrGI^{IMB211}$	23.82	0.10	24	0.013*
$BrGI^{R500}$	20.51	0.08	24	<0.0001*
$BrGI^{IMB211(R500)}$	20.48	0.11	24	<0.0001*
$BrGI^{R500(IMB211)}$	24.14	0.15	22	0.911*
$BrGI^{IMB211(S264A)}$	20.50	0.13	24	<0.0001*
$BrGI^{R500(A264S)}$	25.13	0.10	24	<0.0001*
gi-201	24.27	0.07	24	—
Flowering time of *Arabidopsis gi-201* transformed with *BrGI* alleles: Day of the first flower opening (Fig. 3*A*)				
Col-0	27.38	0.21	58	<0.0001*
$BrGI^{IMB211}$	27.31	0.29	29	<0.0001*
$BrGI^{R500}$	27.18	0.26	51	<0.0001*
$BrGI^{IMB211(R500)}$	27.41	0.31	29	<0.0001*
$BrGI^{R500(IMB211)}$	27.43	0.28	28	<0.0001*
$BrGI^{IMB211(S264A)}$	27.68	0.37	38	<0.0001*
$BrGI^{R500(A264S)}$	26.95	0.26	42	<0.0001*
gi-201	51.21	0.52	39	—
Flowering time of *Arabidopsis gi-201* transformed with *BrGI* alleles: No. of rosette leaves at time of first flower opening (Fig. S3*A*)				
Col-0	9.86	0.14	50	<0.0001*
$BrGI^{IMB211}$	9.36	0.12	47	<0.0001*
$BrGI^{R500}$	9.89	0.10	47	<0.0001*
$BrGI^{IMB211(R500)}$	9.65	0.12	49	<0.0001*
$BrGI^{R500(IMB211)}$	9.69	0.11	49	<0.0001*
$BrGI^{IMB211(S264A)}$	9.63	0.13	41	<0.0001*
$BrGI^{R500(A264S)}$	9.35	0.14	34	<0.0001*
gi-201	39.80	0.35	59	—
Hypocotyl length in red light (cRL) of *Arabidopsis gi-201* transformed with *BrGI* alleles (Fig. 3*B*)				
Col-0	0.33	0.01	21	< 0.0001*
$BrGI^{IMB211}$	0.31	0.01	20	< 0.0001*
$BrGI^{R500}$	0.44	0.02	24	0.247*
$BrGI^{IMB211(R500)}$	0.44	0.02	22	0.377*
$BrGI^{R500(IMB211)}$	0.30	0.01	20	< 0.0001*
$BrGI^{IMB211(S264A)}$	0.43	0.01	22	0.240*
$BrGI^{R500(A264S)}$	0.32	0.01	18	< 0.0001*
gi-201	0.48	0.02	21	—
Hypocotyl length in blue light (cBL) of *Arabidopsis gi-201* transformed with *BrGI* alleles (Fig. S3*B*)				
Col-0	0.18	0.01	18	<0.0001*
$BrGI^{IMB211}$	0.19	0.00	30	<0.0001*
$BrGI^{R500}$	0.21	0.01	37	<0.0001*
$BrGI^{IMB211(R500)}$	0.21	0.01	28	<0.0001*
$BrGI^{R500(IMB211)}$	0.18	0.00	31	<0.0001*
$BrGI^{IMB211(S264A)}$	0.21	0.01	28	<0.0001*
$BrGI^{R500(A264S)}$	0.19	0.01	28	<0.0001*
gi-201	0.24	0.00	29	—
Freezing tolerance (EL50, °C) of *Arabidopsis gi-201* transformed with *BrGI* alleles (Fig. 3*C*)				
Col-0	−7.63	0.29	4	0.150*
$BrGI^{IMB211}$	−6.87	0.20	4	0.003*
$BrGI^{R500}$	−8.51	0.17	4	0.991*
$BrGI^{IMB211(R500)}$	−8.63	0.37	4	0.999*
$BrGI^{R500(IMB211)}$	−7.13	0.38	4	0.013*
$BrGI^{IMB211(S264A)}$	−8.06	0.39	4	0.617*
$BrGI^{R500(A264S)}$	−6.95	0.25	4	0.005*
gi-201	−8.86	0.37	4	—
Salt tolerance of *Arabidopsis gi-201* transformed with *BrGI* alleles (ratio of seedling fresh weight ± 0.15 mM NaCl) (Fig. 3*D*)				
Col-0	0.47	0.07	10	0.017*
$BrGI^{IMB211}$	0.53	0.05	5	0.108*
$BrGI^{R500}$	0.82	0.14	13	0.823*
$BrGI^{IMB211(R500)}$	0.89	0.17	15	0.799*

Table S1. Cont.

	Mean	SEM	*n*	*P*
BrGI$^{R500(IMB211)}$	0.55	0.06	16	0.018*
gi-201	0.83	0.08	15	—
gl1	0.54	0.07	9	0.059*
sos1-1	0.18	0.03	11	<0.0001*
%N/leaf dry mass (g/g) of *Arabidopsis gi-201* transformed with *BrGI* alleles (Fig. S3*C*)				
Col-0	4.93	0.2	15	0.015*
BrGI^{IMB211}	5.08	0.18	21	0.002*
BrGI^{R500}	4.56	0.21	17	0.231*
BrGI$^{IMB211(R500)}$	4.68	0.18	17	0.102*
BrGI$^{R500(IMB211)}$	5.20	0.21	21	0.003*
BrGI$^{IMB211(S264A)}$	5.41	0.12	20	0.0001*
BrGI$^{R500(A264S)}$	4.96	0.18	13	0.014*
gi-201	4.23	0.19	15	—
Water use efficiency (delta 13C) of *Arabidopsis gi-201* transformed with *BrGI* alleles (Fig. S3*D*)				
Col-0	−30.3	0.10	15	0.608*
BrGI^{IMB211}	−30.38	0.12	21	0.212*
BrGI^{R500}	−30.09	0.10	17	0.999*
BrGI$^{IMB211(R500)}$	−30.11	0.12	18	0.996*
BrGI$^{R500(IMB211)}$	−30.39	0.08	21	0.186*
BrGI$^{IMB211(S264A)}$	−30.59	0.11	20	0.006*
BrGI$^{R500(A264S)}$	−30.28	0.14	13	0.737*
gi-201	−29.99	0.12	15	—
Rosette diameter (cm) of *Arabidopsis gi-201* transformed with *BrGI* alleles (Fig. S3*E*)				
Col-0	6.88	1.32	15	0.996*
BrGI^{IMB211}	7.05	1.12	21	0.924*
BrGI^{R500}	6.87	1.10	17	0.997*
BrGI$^{IMB211(R500)}$	6.90	1.20	18	0.993*
BrGI$^{R500(IMB211)}$	6.19	0.91	21	0.952*
BrGI$^{IMB211(S264A)}$	6.31	0.86	20	0.994*
BrGI$^{R500(A264S)}$	6.56	1.32	13	>0.999*
gi-201	6.60	0.85	15	—
Flowering time of *B. rapa gi* mutants (Fig. 4*B*)				
R-*o*-18	27.84	2.27	25	—
gi-1	81.20	5.19	15	<0.0001†
gi-3	77.88	19.18	16	<0.0001†
Circadian period of *B. rapa gi* mutants (Fig. 4*E*)				
R-*o*-18/18 °C	24.00	0.70	21	—
gi-1/18 °C	23.47	0.72	20	0.051†
gi-3/18 °C	23.60	0.84	12	0.2418†
R-*o*-18/22 °C	25.61	1.16	35	—
gi-1/22 °C	27.87	3.65	10 (22 arrhythmic)	0.012†
gi-3/22 °C	28.30	2.86	14 (19 arrhythmic)	0.001†
Freezing tolerance (EL50, °C) of *B. rapa gi* mutants (Fig. 4*F*)				
R-*o*-18	−5.56	0.49	3	—
gi-1	−7.75	0.11	3	0.003†
gi-3	−7.04	0.66	3	0.022†
Salt tolerance (ratio of growth + 200mMol NaCl/growth without NaCl) of *B. rapa gi* mutants (Fig. 4*G*)				
R-*o*-18	0.48	0.18	44	—
gi-1	0.66	0.24	37	0.0003†
gi-3	0.65	0.29	35	0.001†

Summary of phenotypic characterization of *B. rapa* HILs, *BrGI*-transformed *Arabidopsis* lines, and *B. rapa gi* mutants. Circadian period (mean, SEM) calculated by fast Fourier transform-nonlinear least squares (1). *P* is the probability the given value differs from the indicated genotype as determined by Student's *t* test (less than three comparisons) or by ANOVA followed by Tukey's test (three or more comparisons).

*vs. *gi-201*.

†vs. R-*o*-18.

1. Plautz JD, et al. (1997) Quantitative analysis of *Drosophila period* gene transcription in living animals. *J Biol Rhythms* 12(3):204–217.

Table S2. Oligonucleotide primers (shown 5′ to 3′) used in this study

	Primer
For constructs	
Br_GI_locus_F1	CTCCACGTATGGTTTAGAGCCCATC
Br_GI_locus_R1	GAATATGATTGCGTTAGTCACTCATC
I-S1F2	TCTCGGTACGAGACTGCTACGTTAACAG
RI-S1R2	AACTTCATCATCACAAACACTCAGTATGAC
R-S1F2	GCTCGGTACGAGACTGCTACGCTAACAG
For genotyping	
Br_TillingF	AGAGCTCAAGCCACCTACCA
Br_TillingR	TAGAAGTCTCTGGCGGGAAA
Br_Seq1F	GTGTGGGCCTTATGTGTAGTCTTG
Br_Seq1R	CAAGACTACACATAAGGCCCACAC
Br_Seq2F	GCCTCTCACACCCAAGTGCACACG
Br_Seq2R	CGTGTGCACTTGGGTGTGAGAGGC
Br_Seq3F	GATGGCCATGGGGACATGGAG
Br_Seq3R	CTCCATGTCCCCATGGCCATC
Br_Seq4F	CAGCAAAAGCAGCTGCAGCCGTTG
Br_Seq4R	CAACGGCTGCAGCTGCTTTTGCTG
Br_Seq5F	GTATCTACAGGAAGGAGC
Br_Seq5R	GCTCCTTCCTGTAGATAC
Br_Seq6F	CAGCAGCAGGGTTTGGTAC
Br_Seq6R	GTACCAAACCCTGCTGCTG
Br_Seq7R	GTAGTATATCACTGATCCATG
Br_Seq8F	GTTGCTGTCCCTGCACTTCTC
Br_Seq9F	GCTAAGCCAAGCTGAGGGAG
Br_Seq9R	CTCCCTCAGCTTGGCTTAGC
Br_Seq10F	GGAGTCCTTCCGAAGCATGC
Br_Seq10R	GCATGCTTCGGAAGGACTCC
For fine mapping	
KBrB044E18_F	ATGGCGGGTGTAAAACTCTG
KBrB044E18_R	CACCTACTTGTTTCCATCCAA
KBrB049N17_F	GATGGAGAGTGGGTTGTGCT
KBrB049N17_R	CCCAATGAAAGCCATTATCG
KBrS002B15_F	CATCTCCATCCATCACATGC
KBrS002B15_R	CAAACAGGCACGACAATCAT
KBrB020D15_F	GTTGTCAATGTTCGTTCAAA
KBrB020D15_R	AATTAAACAACCACAATAACCA
KBrB048C04_F	CATGGTCGGCTCAAGAATTT
KBrB048C04_R	ACAGCTAAGCGGGGATAAGC
KBrH013B21_F	GTTGTGTGAAATCGCTCAAAT
KBrH013B21_R	GAGTACCACCCAAACCGAAC
KBrH015M19_F	TACCCACGTTGGCAGATGTA
KBrH015M19_R	TCAATTTGGTTTCGGTTAAGTTT
KBrB089L03_F	CCTCCATCAAGCTTCTCTGC
KBrB089L03_R	TCTAACGCCTCCGATTTCAC
KBrH143H14_F	CTCCACGCAAAACCAAAACT
KBrH143H14_R	CGATTCATGGAATTGGAAGG
KBrS010I09_F	CAGATGGGGCCAAGTTACAT
KBrS010I09_R	ACACCGATTTGAAGGCAAAC
KBrB016K20_F	GATTGGGCTGGCTTGTAAGA
KBrB016K20_R	GTTATTTTTGCATTAGATTGAATTTG
KBrB034P04_F	CTCTTGGCTGCAAGGTAAGG
KBrB034P04_R	TCCCTCAGTTAACTTTCTCCACA
KBrB063M04_F	GAGAAATGCCCGTCTGGTAA
KBrB063M04_R	AATGCCTCCATTGTCCTCTG
For qRT-PCR	
Br_RT_Seq7F	CATGGATCAGTGATATACTAC
Br_RT_Seq8R	GAGAAGTGCAGGGACAGCAAC
TUB3-F	TGGTGGAGCCTTACAACGCTACTT
TUB3-R	TTCACAGCAAGCTTACGGAGGTCA